34th EPS Conference on Plasma Phys. Warsaw, 2 - 6 July 2007 ECA Vol.**31F**, P-2.083 (2007)

# Instability of drift-Alfvén wave in collisional solar atmosphere

J. Vranjes[1,2], S. Poedts[1]

[1]*Center for Plasma Astrophysics, Celestijnenlaan 200B, 3001 Leuven, Belgium.*

[2]*Faculté des Sciences Appliquées, avenue F.D. Roosevelt 50, 1050 Bruxelles, Belgium*

In the present work we apply the basic theory of the EM drift wave to the solar plasma. This implies high and equal electron and ion temperatures, and possibly short scales in the perpendicular direction. Therefore, we include the ion gyro-viscosity stress tensor terms which, for short wave lengths, appear of the same order as the standard polarization drift terms.

We assume a magnetic field in the $z$-direction, $B_0\vec{e}_z$, and an equilibrium plasma density that has a gradient in the perpendicular direction. The momentum equations are

$$m_i n_i\left[\frac{\partial\vec{v}_i}{\partial t}+(\vec{v}_i\cdot\nabla)\vec{v}_i\right]=en_i\left(-\nabla\phi-\frac{\partial A_z}{\partial t}\vec{e}_z+\vec{v}_i\times\vec{B}\right)-\kappa T_i\nabla n_i-\nabla\cdot\Pi_i-m_i n_i\nu_i\vec{v}_i, \quad (1)$$

$$m_e n_e\left[\frac{\partial\vec{v}_e}{\partial t}+(\vec{v}_e\cdot\nabla)\vec{v}_e\right]=-en_i\left(-\nabla\phi-\frac{\partial A_z}{\partial t}\vec{e}_z+\vec{v}_e\times\vec{B}\right)-\kappa T_e\nabla n_e-\nabla\cdot\Pi_e-m_e n_e(\nu_e\vec{v}_e-\nu_{ei}\vec{v}_i). \quad (2)$$

Here, $\nu_i\equiv\nu_{in}$ and $\nu_e=\nu_{en}+\nu_{ei}$. The parallel electron dynamics is described by

$$\left(\frac{\partial}{\partial t}+\vec{v}_{e0}\nabla_\perp\right)A_{z1}+\frac{\partial\phi_1}{\partial z}-\frac{\kappa T_e}{n_{e0}e}\frac{\partial n_{e1}}{\partial z}-\frac{m_e\nu_e}{\mu_0 e^2 n_{e0}}\nabla_\perp^2 A_{z1}=0. \quad (3)$$

Here, $\vec{v}_{e0}=-\kappa T_e\vec{e}_z\times\nabla_\perp n_{e0}/(eB_0n_{e0})$. The electron continuity becomes

$$\frac{\partial n_{e1}}{\partial t}+\frac{1}{B_0}(\vec{e}_z\times\nabla_\perp\phi_1)\cdot\nabla_\perp n_{e0}+\frac{1}{\mu_0 e}\frac{\partial}{\partial z}\nabla_\perp^2 A_{z1}=0. \quad (4)$$

The ion continuity is combined with Eq. (4) yielding

$$\left(\frac{\partial}{\partial t}+\nu_i\right)\nabla_\perp^2\phi_1+c_a^2\frac{\partial}{\partial z}\nabla_\perp^2 A_{z1}+\frac{\kappa T_i}{en_0}\left(\frac{\partial}{\partial t}+\nu_i\right)\nabla_\perp^2 n_1-\rho_i^2\frac{\partial}{\partial t}\nabla_\perp^4\left(\phi_1+\frac{\kappa T_i}{en_0}n_1\right)=0. \quad (5)$$

Here, $\rho_i=v_{Ti}/\Omega_i$, and $v_{Ti}^2=\kappa T_i/m_i$. The given set of equations (3), (4), and (5) will be used in the description of the drift-Alfvén waves in solar plasma. In Cartesian geometry, for perturbations $\sim\exp(-i\omega t+ik_y y+ik_z z)$, Eqs. (3), (4), and (5) yield

$$\omega^3-\omega^2\left[\omega_{*e}+\omega_{*i}-i\left(\delta+\frac{\nu_i}{1+k_y^2\rho_i^2}\right)\right]+\omega\left\{\omega_{*e}\omega_{*i}-\frac{k_z^2c_a^2}{1+k_y^2\rho_i^2}-k_y^2k_z^2c_a^2(\rho_s^2+\rho_i^2)-\frac{\nu_i\delta}{1+k_y^2\rho_i^2}\right.$$
$$\left.-i\left[\omega_{*i}\delta+\frac{\nu_i(\omega_{*e}+\omega_{*i})}{1+k_y^2\rho_i^2}\right]+\frac{\omega_{*e}k_z^2c_a^2}{1+k_y^2\rho_i^2}+\frac{\omega_{*i}\nu_i\delta}{1+k_y^2\rho_i^2}\right\}+i\frac{\nu_i}{1+k_y^2\rho_i^2}\left[\omega_{*e}\omega_{*i}-k_z^2c_a^2k_y^2\left(\rho_s^2+\rho_i^2\right)\right]=0. \quad (6)$$

Here, $\omega_{*e}=k_y v_{e0}$, $\omega_{*i}=k_y v_{i0}$, $\delta=m_e\nu_e k_y^2/(\mu_0 n_0 e^2)$. We solve Eq. (6) numerically by taking parameters typical for the solar corona, viz. $T_e=T_i=1.5\cdot10^6$ K, $n_{e0}=n_{i0}=10^{14}$ m$^{-3}$, and

taking $B_0 = 10^{-3}$ T. We calculate the spectrum for the two oppositely propagating Alfvén modes and the drift mode. For these parameters we obtain $\nu_{ei} \simeq 2.1$ Hz, $\nu_{ii} \simeq 0.07$ Hz, $c_s = 1.11 \cdot 10^5$ m/s, $c_a = 2.18 \cdot 10^6$ m/s, $v_{Te} = 4.77 \cdot 10^6$ m/s, $\beta = 0.0052 > m_e/m_i = 0.00054$.

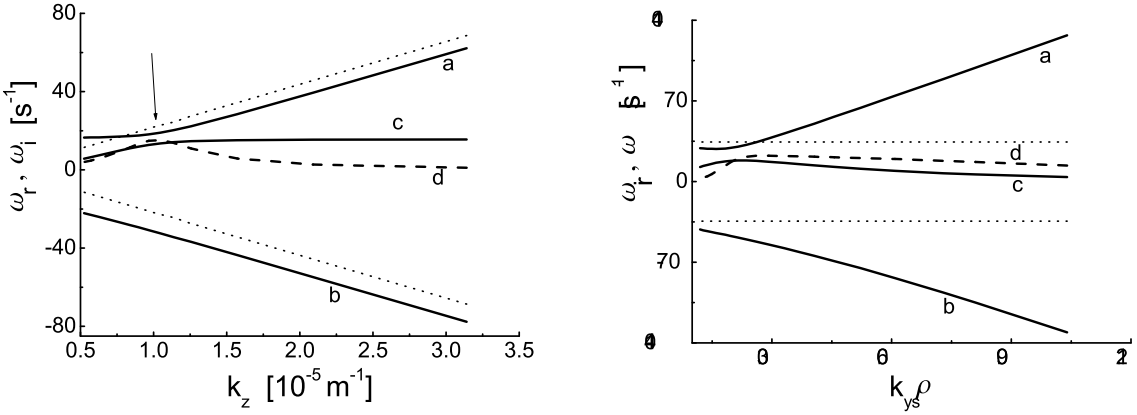


Figure 1: Left: Frequencies $\omega_r$ and increment $\omega_i$ of electromagnetic the drift-Alfvén perturbations with the effect of the coupling between the Alfvén (lines $a$ and $b$) and drift (line $c$) parts. Dotted lines denote $\pm k_z c_a$. The increment of the electrostatic drift mode (multiplied by $10^3$) has a maximum in the region where the retarded kinetic-Alfvén mode and the drift mode change their identities (denoted by arrow). Right: Frequencies $\omega_r$ and increment $\omega_i$ of the drift-Alfvén perturbations in terms of the coupling term $k_y\rho_s$. The drift wave increment (line $d$) is multiplied by $10^3$. Dotted lines denote $|k_z c_a| = 34.3$ Hz.

The behavior of the modes in terms of the parallel wave-number $k_z$ is presented in Fig. 1 (left) for $L_n = 10^3$ m and $\lambda_y = 50$ m, while $k_y\rho_s = 0.15$. We thus have two (retarded and accelerated) damped kinetic-Alfvén modes, lines $a$ and $b$, respectively, and an electrostatic drift mode (line c). The increment of the drift mode (multiplied by $10^3$) is presented by line $d$. The drift mode is unstable in the whole range of wave-numbers. Its frequency is nearly constant for large values of $k_z$. In the area denoted by the arrow, the retarded kinetic-Alfvén mode and the drift mode do not cross each other. Instead, they change identities as typical for an 'avoided crossing'. For observations, the low frequency (small $k_z$) domain is of particular importance as this parameter can be measured, i.e. spatially resolved. It is clearly seen in Fig. 1 that, in fact, this is the domain in which the Alfvén mode frequency can be very different from what is expected or predicted if the small-scale plasma inhomogeneity, which drives the drift mode, is neglected. Here, for the given density scale length, the two frequency limits at $k_z \to 0$ are $\pm 16.26$ Hz. Clearly, the frequencies can be made arbitrary small by changing the equilibrium density scale length $L_N$. The decrement of the Alfvén modes has also been calculated and, in general, the accelerated

mode $b$ is less damped. Its damping rate changes between $-3.5\cdot 10^{-3}$ Hz at $k_z = 3.14$ (in given units), and $-1.1\cdot 10^{-3}$ Hz at $k_z = 0.5$. The damping rate of the decelerated mode $a$ has a maximum absolute value of about $2.3\cdot 10^{-2}$ Hz.

In Fig. 1 (right) we present the mode behavior in terms of the coupling term $k_y\rho_s$ for a fixed value of $|k_z c_a| = 34.3$ Hz (presented by dotted lines). The notation corresponds to the one used in Fig. 1 (left). Note that at $k_y\rho_s = 1$ the frequencies of the two kinetic-Alfvén modes are around 127 and $-131$ Hz. Thus, the actual frequencies may drastically differ from what is expected without the drift mode.

In order to present the mode behavior in magnetic structures that are highly elongated along the magnetic field lines and localized in the perpendicular direction, we shall rewrite the starting equations in cylindric coordinates. The combined electron dynamics equations (3) and (4) yield:

$$\left(\nabla_\perp^2 + \frac{\frac{\omega\omega_2}{c_a^2 k_z^2\rho_s^2}}{1-\frac{i\nu_e\omega}{k_z^2 v_{Te}^2}}\right)\widehat{A}_{z1} - \frac{1}{k_z c_a^2}\frac{\frac{\omega}{\rho_s^2}+\frac{m\Omega_i}{r}\frac{n_0'}{n_0}}{1-\frac{i\nu_e\omega}{k_z^2 v_{Te}^2}}\widehat{\phi}_1 = 0, \tag{7}$$

where $\omega_2 = \omega - v_{e0}(r)m/r$, and $\nabla_\perp = \partial^2/\partial r^2 + \partial/(r\partial r) - m^2/r^2$. The ion part can be discussed in two limits. In the limit of negligible ion thermal effects from Eq. (5) we obtain $\nabla_\perp^2\widehat{\phi}_1 - (k_z^2 c_a^2/\omega)\nabla_\perp^2\widehat{A}_{z1} = 0$, which is used in Eq. (7) yielding

$$\nabla_\perp^2\left[\left(\nabla_\perp^2 - \frac{1}{\omega(1-i\delta_1)}\left(\frac{\omega}{\rho_s^2}+\frac{m\Omega_i}{r}\frac{n_0'}{n_0}\right)\right)\widehat{\phi}_1\right] + \nabla_\perp^2\left[\frac{\omega - mv_{e0}/r}{k_z\rho_s^2(1-i\delta_1)}\widehat{A}_{z1}\right] = 0. \tag{8}$$

To further decouple the equations for the potentials we assume $n_0(r) = N_0\exp(ar^2/2)$, where $a$ can be both positive and negative, and $r$ takes values between 0 and $r_0$. All the terms under the operators in this case become constant and Eq. (8) becomes of the form

$$\nabla_\perp^2\left\{\left[\nabla_\perp^2 - \frac{\omega/\rho_s^2 + am\Omega_i}{\omega(1-i\delta_1)} + \frac{\omega(\omega + am\kappa T_e/eB_0)}{k_z^2\rho_s^2 c_a^2(1-i\delta_1)}\right]\widehat{\phi}_1\right\} = 0. \quad \text{or} \quad \nabla_\perp^2\psi(r) = 0. \tag{9}$$

Here, consequently $\psi(r) = 0$, or $\psi(r) = c_1\cosh[m\log(r)] + c_2\sinh[m\log(r)]$ and we have

$$\left(\frac{\partial^2}{\partial r^2} + \frac{1}{r}\frac{\partial}{\partial r} - \frac{m^2}{r^2} + \xi^2\right)\left[\widehat{\phi}_1 - \frac{\psi(r)}{\xi^2}\right] = 0, \tag{10}$$

where

$$\xi^2 = \frac{\omega(\omega+\omega_0)}{\rho_s^2(1-i\delta)}\left(\frac{1}{c_a^2 k_z^2} - \frac{1}{\omega^2}\right), \quad \omega_0 = am\frac{\kappa T_e}{eB_0}, \quad \delta_1 = \frac{\nu_e\omega}{k_z^2 v_{Te}^2}.$$

The solutions of Eq. (10) are the Bessel functions of the first and the second kind, $J_n(\xi r)$ and $Y_n(\xi r)$, with a complex argument. For nonsingular eigen-functions we keep $J_n(\xi r)$ and we have, first that if $n > -1$, then the zeros of the Bessel function $J_n(z)$ with the complex argument $z$ are all real, and, second, for $n \geq 0$ the functions $J_n(z)$ and $J_{n+s}(z)$ have no common zeros

other than the origin, for all $s > 0$. Hence, for vanishing solutions at the boundary, we set that $\xi r_0 = \varepsilon_l$ where $\varepsilon_l$ is the real $l$-th zero of the complex function $J_n(\xi r)$. This allows us to write the dispersion equation for the radially bounded plasma

$$\left(\omega + am\frac{\kappa T_e}{eB_0}\right)(\omega^2 - k_z^2 c_a^2) = \omega k_z^2 c_a^2 \frac{\varepsilon_l^2 \rho_s^2}{r_0^2}(1 - i\delta). \tag{11}$$

Here both $m$ and $\varepsilon_l$ take given discrete values. Eq. (11) describes the global drift-Alfvén wave, with an unstable drift wave part. The poloidal (i.e. in the $\theta$-direction) propagation is the consequence of the drift mode which propagates perpendicular to both the magnetic field lines and the density gradient. Combined with the given $z$-dependence, this gives the twisting of the global modes, which vanishes for $m = 0$ when the two modes decouple.

Keeping the ion thermal effects the procedure can be repeated yielding the solutions as the Bessel functions of the first kind, and the corresponding dispersion equation which reads

$$\eta^2 = \frac{\varepsilon_l^2}{r_0^2}. \tag{12}$$

Here,

$$\eta^2 = \left[\omega(\omega + i\nu_i)\left(\omega + ma\rho_s^2\Omega_i\right)\left(\omega - ma\rho_i^2\Omega_i\right)\right.$$
$$\left. -\omega k_z^2 c_a^2\left(\omega + ma\rho_s^2\Omega_i\right)\right]\left\{k_z^2 c_a^2(\omega + i\nu_i)\left[\rho_s^2(1 - i\delta_1)\left(\omega - ma\rho_i^2\Omega_i\right) + \rho_i^2(\omega + ma\rho_s^2\Omega_i)\right]\right\}^{-1}.$$

The solutions of Eq. (12) describe the eigen-values of the global eigen-modes in the given cylindrical plasma. Mode details are available in Refs. [2], [3]. Eq. (12) can be easily solved numerically for various harmonics by choosing the appropriate $\varepsilon_l$ and $m$. In the case of solar coronal magnetic structures, the density and the magnetic field have higher values compared to the previous case $n_{i0} = n_{e0} = 10^{16}$ m$^{-3}$ and $B_0 \simeq 10^{-2}$ T. Taking as an example a magnetic column with the diameter of 200 km and, in the case when the density at its edge is 0.1 of its value at the column axis, we get $a \simeq 7 \cdot 10^{-10}$ m$^{-2}$, and therefore, the poloidal mode number $m$ takes very high values $\sim 10^5$.

## References

[1] J. Weiland, *Collective Modes in Inhomogeneous Plasmas* (Institute of Physics Pub., Bristol 2000).

[2] J. Vranjes and S. Poedts, Phys. Plasmas **13**, 032107 (2006).

[3] J. Vranjes and S. Poedts, Astron. Astropphys. **458**, 635 (2006).